General Disclaimer

One or more of the Following Statements may affect this Document

- This document has been reproduced from the best copy furnished by the organizational source. It is being released in the interest of making available as much information as possible.

- This document may contain data, which exceeds the sheet parameters. It was furnished in this condition by the organizational source and is the best copy available.

- This document may contain tone-on-tone or color graphs, charts and/or pictures, which have been reproduced in black and white.

- This document is paginated as submitted by the original source.

- Portions of this document are not fully legible due to the historical nature of some of the material. However, it is the best reproduction available from the original submission.

DRF-9617

MECHANICAL

TECHNOLOGY

INCORPORATED

Mechanical Technology Incorporated
968 Albany Shaker Road
Latham, New York 12110

MTI-69TR7

ANALYSIS, DESIGN AND PROTOTYPE DEVELOPMENT OF SQUEEZE-FILM BEARINGS FOR AB-5 GYRO

PHASE VI FINAL REPORT

ANALYTICAL INVESTIGATION ON DYNAMIC RESPONSES AND START-UP PROCESS OF SQUEEZE-FILM BEARINGS

by

T. Chiang
C.H.T. Pan

April 30, 1969

TECHNICAL REPORT

NO. MTI-69TR7

DATE: April 1969

ANALYSIS, DESIGN AND PROTOTYPE DEVELOPMENT OF SQUEEZE-FILM BEARINGS FOR AB-5 GYRO
PHASE VI FINAL REPORT
ANALYTICAL INVESTIGATION ON DYNAMIC RESPONSES AND START-UP PROCESS OF SQUEEZE-FILM BEARINGS

by

T. Chiang
C.H.T. Pan

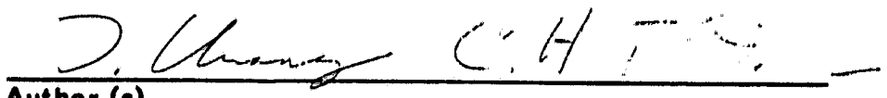

Author (s)

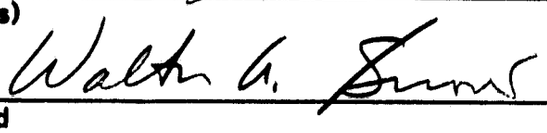

Approved

Approved

Prepared for

National Aeronautics and Space Administration
George C. Marshall Space Flight Center
Huntsville, Alabama

Prepared under

Contract: NAS 8-11678

MTI
MECHANICAL TECHNOLOGY INCORPORATED

968 ALBANY - SHAKER ROAD — LATHAM, NEW YORK — PHONE 785-0922

TABLE OF CONTENTS

FOREWORD

Mechanical Technology Incorporated has been under contract with George C. Marshall Space Flight Center, NASA, to conduct a project entitled, "Analysis, Design and Prototype Development of Squeeze Film Bearings for AB-5 Gyro". The main objective of this Phase (VI) is to investigate analytically the dynamic responses of squeeze-film bearings and the start-up process of a squeeze-film thrust plate.

This report contains two parts:

I. Summary on Phase VI Work

II. Topical Report on "Synchronous Responses of Spherical and Conical Squeeze-Film Bearing Systems".

PART I

SUMMARY ON PHASE VI WORK

The main objective of Phase VI is to investigate analytically the dynamic responses and the start-up process of squeeze-film bearings.

In the literature, analytical investigations were performed on squeeze-film bearings [1 to 6] by assuming that the supported mass be stationary disregarding the oscillatory forces imposed by the squeeze action. In reality the supported mass may respond dynamically with the squeeze action. This was investigated analytically in [7] by a simplified approach with the response assumed to be synchronous. The results indicate that the load capacity may be considerably affected by the synchronous response depending on the squeeze frequency and the mass of the float.

The supported mass motion was also studied in [8]. For moderately high squeeze number, numerical solution for the response was obtained using small perturbation analysis. The supported mass respond was found to be synchronous with the squeeze motion; this was also verified by experimental observation. The dynamic response of a spherical squeeze-film bearing with a time scale much larger than that of the squeeze motion was investigated in [10] using the results of [11].

Three topical reports have been issued under this phase of the contract.

1) "Dynamic Responses of a Double Squeeze-Film Thrust Plate", by T. Chiang, C.H.T. Pan and H. G. Elrod, Report MTI-68TR56, 1968.

2) "Synchronous Responses of Spherical and Conical Squeeze-Film Bearing System" by T. Chiang and C.H.T. Pan, Report MTI-69TR7, 1969.

3) "On the Start-Up Process in a Gaseous Squeeze-Film Thrust Circular Disk", by T. Chiang, C.H.T. Pan and V. Castelli, Report MTI-69TR16, 1969.

The first topical report, listed as Ref. [9], investigates the dynamic responses of squeeze-film bearings with very high squeeze number. The geometry of a double squeeze-film circular disk has been chosen for simplicity. The results show that the dynamic response is mainly synchronous and sub-harmonic responses are negligibly small in magnitude. When the squeeze frequency is high (large B with $B = \frac{MC\Omega^2}{\pi R^2 p_a}$), the response is 180° out-of-phase with the squeeze action. This enhances the squeeze action, and thus increases the load capacity and stiffness. The converse is true for low squeeze frequency (small B). In normal operating condition of a squeeze film bearing, the large B criterion is easily satisfied. However, when B is very large, the magnitude of the response becomes negligibly small that the supported mass in essentially stationary. Three methods of solution have been used to solve the problem, namely, linearized harmonic analysis, non-linear harmonic analysis and the exact numerical solution. The last method gives the best results but it is time-consuming.

The results of the linearized harmonic analysis are only qualitatively correct. The non-linear harmonic analysis appears to be a best compromise; it yields results in good agreement with those of the exact numerical solution, and it is relatively easy to handle analytically.

The second topic report, entitled, "Synchronous Responses of Spherical and Conical Squeeze-Film Bearing Systems", is included in this report. The configurations shown in Fig. 1 and Fig. 2 are motivated by a new transducer design for Phase V of this contract. This new transducer is for squeeze-film bearing support of a line AB-5 gyro float. The gyro wheel supported by its bearing is considered to be one mass, whereas the squeeze-film journals (spherical or conical) connected by a rigid shaft is considered as a second mass, and thus constitutes a two-mass system. Because of the previous success, the method of non-linear harmonic analysis was used to analyze the responses of both the float (the journal)

and the gyro wheel. The results show that they display typical behavior of the dynamic responses of a two degree-of-freedom system. The system has two critical frequencies at which the dynamic responses become unbounded. When the squeeze frequency is much higher than the critical frequencies, both the journal and the wheel responses have negligibly small amplitude; the load capacity and stiffness are practically not affected by the synchronous response. In certain frequency range, the response of the journal may result in appreciably higher load capacity and stiffness. But in the mean time, the response of the wheel becomes excessively large. Therefore, one cannot take advantage of this high load capacity characteristics and it is recommended that the squeeze frequency be designed to be sufficiently higher than the critical frequencies.

The third topical report deals with the start-up process of a squeeze-film bearing. Again, a circular disk thrust bearing is chosen for simplicity. It is assumed that separation of the supported mass from the oscillatory bearing surface would occur because the supported mass cannot follow the oscillation motion. We, therefore, transform the actual start-up process into an idealized situation; the supported mass is assumed to start with a given velocity and a given elevation different from the equilibrium film thickness. The analytical results show that when the gap is greater than the equilibrium film thickness, the squeeze film force is not large enough to support the float. Consequently, the gap would decrease. When the gap decreases to a value equal to the equilibrium film thickness, although the squeeze-film force balances out with the load, the gap will continue to decrease because of the inertia of the float. Now the squeeze-film force is building up until it reaches a value that will compensate the float inertia; at that point, the gap ceases to decrease. The squeeze-film force is now too large and the float starts to move up. It will over-shoot the equilibrium position and the process will repeat itself with decreasing amplitude. The float would eventually settle down toward the equilibrium position.

PART II

SYNCHRONOUS RESPONSES OF SPHERICAL AND CONICAL SQUEEZE-FILM BEARING SYSTEMS

1. INTRODUCTION

Gaseous squeeze-film bearings were analyzed in the literature by many investigators [1 to 6]. Asymptotic approximations for large squeeze number were formulated in [2]. In References 3 to 6, the performance of various squeeze-film bearing geometry was given with the assumption that one of the squeeze surfaces is oscillating under a prescribed mode and at a high frequency while the other bearing surface, normally the supported mass, is held stationary. Because of the excitation due to squeeze action, the supported mass may respond dynamically. This was investigated in [7], [8] and [9]. Numerical solution of the supported mass motion was obtained in [8] for moderately high squeeze number; it was found both analytically and experimentally that the supported mass motion is synchronous with the squeeze action. When the squeeze number is very high, the dynamic response of the supported mass was investigated in [7] and [9] using the asymptotic approximation for large squeeze number. In Reference [9] the response of a double squeeze-film thrust plate was determined by using three methods of solution, namely, linearized harmonic solution, non-linear harmonic solution, and exact numerical solution. It was found that the response is predominantly synchronous. Furthermore the non-linear harmonic solution yields results which agree well with the exact numerical solution. In this report, the synchronous responses of spherical and conical squeeze-film bearing systems will be investigated. Because of its previous success, the non-linear harmonic method of solution will be used. Only responses in the axial direction will be considered and the bearing is assumed to be radially unloaded.

The configurations of the spherical and conical squeeze-film bearing systems depicted in Figures 1 and 2 show that an additional spring-mass system is attached to the float. This is motivated, in particular, by the gimbal squeeze-film suspension of a gyro float; the mass would then be the mass of the wheel and k the stiffness of the spin-axis bearing.

2. ANALYSIS OF SPHERICAL BEARING SYSTEM

The spherical bearing system shown in Fig. 1 will be used for analysis. Two opposing spherical segments designated by A and B, are connected by a rigid element on which the gyro wheel is mounted. Assume that the gyro wheel has mass M_W and the spin axis bearing has stiffness k. The analyses for the conical geometry can be carried out in a similar manner; they are included in Appendix I.

In the spherical coordinate system, denote the meridianal and azimuthal angles by θ and φ respectively. The azimuthal angle is illustrated in Fig. 1. Since the squeeze-film bearings are assumed to be radially unloaded, there is no θ dependence. The transducers for the arrangement shown in Fig. 1 are normally operated in a symmetrical fashion so that the normalized squeeze actions of both squeeze surfaces "A" and "B" can be represented by $b(\varphi)\cos\tau$, where $b(\varphi)$ is a mode function. Assume that the response of the float is synchronous and can be represented by $\epsilon \cos\tau$. This approach was successful in dealing with the double squeeze-film thrust plate [9] and will be applied again here. Note that both spherical segments have the same response $\epsilon \cos\tau$, because they are assumed to be connected by a rigid element. Let η_A and η_B be the normalized steady-state displacements of journals "A" and "B" from their concentric position; both are defined to be positive upwards. The normalized film thicknesses can now be written as

$$H_A = 1 + \eta_A \cos\varphi + [\epsilon \cos\varphi - b(\varphi)] \cos\tau \qquad (1)$$

$$H_B = 1 - \eta_B \cos\varphi + [-\epsilon \cos\varphi - b(\varphi)] \cos\tau \qquad (2)$$

Note that the quantities H_A, η_A, ϵ, $b(\varphi)$ etc. have been normalized with respect to the bearing clearance C.

The isothermal Reynolds' equation of a spherical squeeze-film bearing is (Ref. 4),

$$\frac{1}{\sin\varphi}\frac{\partial}{\partial\varphi}\left[\sin\varphi\, H^3\, P\,\frac{\partial P}{\partial\varphi}\right] = \sigma\,\frac{\partial}{\partial\tau}(PH) \tag{3}$$

where

$$P = \frac{p}{p_a}$$

$$\sigma = \frac{12\mu\Omega}{p_a}\left(\frac{R}{C}\right)^2 = \text{squeeze number}$$

$$\Omega = \text{squeeze frequency}$$

$$\tau = \Omega t$$

Equation (3) is obviously applicable to either bearing "A" or bearing "B", and H can be interpreted as H_A or H_B accordingly. For large σ, the asymptotic approximation of (3) is, from Ref. 4,

$$\frac{d}{d\varphi}\left[\sin\varphi\,\frac{d}{d\varphi}(H_o\,\psi_\infty^2) - 3\,\psi_\infty^2\sin\varphi\,\frac{dH_o}{d\varphi}\right] = 0 \tag{4}$$

where

$$\left.\begin{aligned}\psi_\infty &= \lim_{\sigma\to\infty}(PH)\\ H_o &= \frac{1}{2\pi}\int_0^{2\pi} H\,d\tau\end{aligned}\right\} \tag{5}$$

The boundary conditions as derived from a Mass Content Rule in Reference 4, are

$$\left.\begin{aligned} \psi_\infty^2(\varphi_1) &= \frac{\int_0^{2\pi} H^3(\varphi_1,\tau)\, d\tau}{2\pi H_o(\varphi_1)} \\ \psi_\infty^2(\varphi_2) &= \frac{\int_0^{2\pi} H^3(\varphi_2,\tau)\, d\tau}{2\pi H_o(\varphi_2)} \end{aligned}\right] \qquad (6)$$

Integrate (4) with respect to φ,

$$\sin\varphi \left[\frac{d}{d\varphi}(H_o \psi_\infty^2) - 3\psi_\infty^2 \frac{dH_o}{d\varphi} \right] = E \qquad (7)$$

where E is a constant.

Assume that

$$F(\varphi) = \left(\frac{\psi_\infty}{H_o}\right)^2 \qquad (8)$$

Substituting (8) into (7), we obtain

$$H_o^3 \frac{dF}{d\varphi} = \frac{E}{\sin\varphi}$$

which can be readily integrated to yield

$$F(\varphi) = E \int_{\varphi_1}^{\varphi} \frac{d\varphi'}{H_o^3(\varphi')\sin\varphi'} + F(\varphi_1) \qquad (9)$$

Equation (9) can of course be used for bearing "A" or "B". For bearing "A", use subscript "A" for the respective quantities and rewrite Eq. (9),

$$F_A(\varphi) = E_A \int_{\varphi_1}^{\varphi} \frac{d\varphi'}{H_{oA}^3(\varphi') \sin \varphi'} + F_A(\varphi_1) \tag{10}$$

Two arbitrary constants, E_A and $F_A(\varphi_1)$, are to be determined by boundary conditions. Combining Equations (6) and (8), we have

$$F_A(\varphi_1) = 1 + \frac{3}{2} \left[\frac{\varepsilon \cos \varphi_1 - b(\varphi_1)}{H_{oA}(\varphi_1)} \right]^2$$

$$F_A(\varphi_2) = 1 + \frac{3}{2} \left[\frac{\varepsilon \cos \varphi_2 - b(\varphi_2)}{H_{oA}(\varphi_2)} \right]^2 \tag{11}$$

From Eq. (10), E_A can be easily obtained by setting $\varphi = \varphi_2$,

$$E_A = \frac{F_A(\varphi_2) - F_A(\varphi_1)}{\int_{\varphi_1}^{\varphi_2} \left[H_{oA}^3 \sin \varphi \right]^{-1} d\varphi} \tag{12}$$

Similarly, for bearing "B",

$$
\left.
\begin{aligned}
F_B(\varphi) &= E_B \int_{\varphi_1}^{\varphi} \frac{d\varphi'}{H_{oB}^3(\varphi') \sin \varphi'} + F_B(\varphi_1) \\
F_B(\varphi_1) &= 1 + \frac{3}{2} \left[\frac{\varepsilon \cos \varphi_1 + b(\varphi_1)}{H_{oB}(\varphi_1)}\right]^2 \\
F_B(\varphi_2) &= 1 + \frac{3}{2} \left[\frac{\varepsilon \cos \varphi_2 + b(\varphi_2)}{H_{oB}(\varphi_2)}\right]^2 \\
E_B &= \frac{F_B(\varphi_2) - F_B(\varphi_1)}{\int_{\varphi_1}^{\varphi_2} \left[H_{oB}^3 \sin \varphi\right]^{-1} d\varphi}
\end{aligned}
\right\} \qquad (13)
$$

Knowing $F_A(\varphi)$ and $F_B(\varphi)$, we can proceed to obtain

$$
\begin{aligned}
\psi_{\infty A} &= H_{oA} \sqrt{F_A(\varphi)} \\
\psi_{\infty B} &= H_{oB} \sqrt{F_B(\varphi)}
\end{aligned} \qquad (14)
$$

The instantaneous film forces in the axial direction, F_{IA} and F_{IB} can be obtained by integrating the pressure above the ambient,

$$
F_{IA} = \int_{\varphi_1}^{\varphi_2} (p_A - p_a)\, 2\pi R^2 \sin \varphi \cos \varphi \, d\varphi \qquad (15)
$$

$$F_{IB} = -\int_{\varphi_1}^{\varphi_2} (p_B - p_a)\, 2\pi R^2 \sin\varphi \cos\varphi \, d\varphi \tag{16}$$

The forces are defined to be positive upwards. Non-dimensionalizing with $\pi R^2 p_a$ and replacing P_A by $\psi_{\infty A}/H_A$ and so on, we have

$$\frac{F_{IA}}{\pi R^2 p_a} = \int_{\varphi_1}^{\varphi_2} \frac{\psi_{\infty A} \sin 2\varphi \, d\varphi}{H_{oA} + [\epsilon \cos\varphi - b(\varphi)]\cos\tau} + \frac{1}{2}(\cos 2\varphi_2 - \cos 2\varphi_1) \tag{17}$$

$$\frac{F_{IB}}{\pi R^2 p_a} = -\int_{\varphi_1}^{\varphi_2} \frac{\psi_{\infty B} \sin 2\varphi \, d\varphi}{H_{oB} + [-\epsilon \cos\varphi - b(\varphi)]\cos\tau} - \frac{1}{2}(\cos 2\varphi_2 - \cos 2\varphi_1) \tag{18}$$

Note that we have used the asymptotic approximation and neglected the edge corrections for the squeeze film forces. In so doing, the damping part of the squeeze action is automatically discarded (See Ref. 9).

Since the squeeze-film forces are exclusively in the axial direction for a radially unloaded bearing, we can write one axial equation of motion for the spherical journal,

$$-M_J C \epsilon \omega^2 \cos\tau = F_{IA} + F_{IB} - W_J - W_W + k C (\delta \cos\tau - \epsilon \cos\tau) \tag{19}$$

where

M_J = mass of the journal

W_J = weight of the journal

W_W = weight of the wheel

k = stiffness of the bearing for wheel

δ = dimensionless amplitude of oscillation of the wheel from its equilibrium position.

Now that we have introduced an additional unknown δ, we need one more equation which is the equation of motion of the wheel. Note that the motion of the wheel was also assumed to be synchronous.

$$- M_W C \delta \omega^2 \cos \tau = - k C (\delta \cos \tau - \epsilon \cos \tau) \tag{20}$$

M_W is the mass of the wheel.

Multiply Eq. (19) and (20) by cos τ and integrate from 0 to 2π,

$$- B_J \epsilon = \frac{1}{\pi} \int_{\varphi_1}^{\varphi_2} d\varphi \int_0^{2\pi} \frac{(\psi_{\infty A} \sin 2\varphi)\cos \tau \, d\tau}{H_{oA} + [\epsilon \cos \varphi - b(\varphi)]\cos \tau}$$

$$- \frac{1}{\pi} \int_{\varphi_1}^{\varphi_2} d\varphi \int_0^{2\pi} \frac{(\psi_{\infty B} \sin 2\varphi)\cos \tau \, d\tau}{H_{oB} + [-b(\varphi) - \epsilon \cos \varphi]\cos \tau}$$

$$+ K \cdot (\delta - \epsilon) \tag{21}$$

$$- B_W \delta = - K \cdot (\delta - \epsilon) \tag{22}$$

where

$$\left.\begin{aligned} B_J &= \frac{M_J C \omega^2}{\pi R^2 p_a} \\ B_W &= \frac{M_W C \omega^2}{\pi R^2 p_a} \\ K &= \frac{kC}{\pi R^2 p_a} \end{aligned}\right\} \tag{23}$$

Equations (21) and (22) are two non-linear equations for ϵ and δ. Iteration

method will be used to obtain the solution starting from a linearized solution as a first guess.

Linearized Solution

For the case that

$$\left.\begin{aligned} \frac{|\epsilon \cos\varphi - b(\varphi)|}{H_{oA}} &\ll 1 \\ \text{and} \\ \frac{|\epsilon \cos\varphi + b(\varphi)|}{H_{oB}} &\ll 1 \end{aligned}\right] \tag{24}$$

Then, Equations (21) and (22) can be linearized to

$$(-B_J + X_A + X_B + K)\,\epsilon - K\,\delta = Y_A + Y_B \tag{25}$$

$$-K\,\epsilon + (-B_W + K)\,\delta = 0 \tag{26}$$

where

$$\left.\begin{aligned} X_A &= \int_{\varphi_1}^{\varphi_2} \frac{\sin 2\varphi \cos\varphi}{H_{oA}}\, d\varphi \\ X_B &= \int_{\varphi_1}^{\varphi_2} \frac{\sin 2\varphi \cos\varphi}{H_{oB}}\, d\varphi \\ Y_A &= \int_{\varphi_1}^{\varphi_2} \frac{\sin 2\varphi\, b(\varphi)}{H_{oA}}\, d\varphi \\ Y_B &= -\int_{\varphi_1}^{\varphi_2} \frac{\sin 2\varphi\, b(\varphi)}{H_{oB}}\, d\varphi \end{aligned}\right] \tag{27}$$

Equations (25) and (26) can be written in matrix form

$$\begin{bmatrix} (-B_J + X_A + X_B + K) & -K \\ -K & (-B_W + K) \end{bmatrix} \begin{bmatrix} \epsilon \\ \delta \end{bmatrix} = \begin{bmatrix} Y_A + Y_B \\ 0 \end{bmatrix}$$

Thus,

$$\begin{bmatrix} \epsilon \\ \delta \end{bmatrix} = \begin{bmatrix} (-B_J + X_A + X_B + K) & -K \\ -K & (-B_W + K) \end{bmatrix}^{-1} \begin{bmatrix} Y_A + Y_B \\ 0 \end{bmatrix} \tag{28}$$

The linearized solution ϵ and δ can be easily obtained from (28). Also, it is seen that the critical frequencies of the system can be readily obtained by setting the determinant of the matrix equal to zero.

$$\left.\begin{aligned} &(-Q_J \omega^2 + X_A + X_B + K)(-Q_W \omega^2 + K) - K^2 = 0 \\ &\text{where} \\ &Q_J = \frac{M_J C}{\pi R^2 p_a} \\ &Q_W = \frac{M_W C}{\pi R^2 p_a} \end{aligned}\right\} \tag{29}$$

Thus, the two critical speeds according to the linearized analysis are

$$\omega_{cr} = \left[\frac{T_1 \pm \sqrt{T_2}}{2Q_J\ Q_W}\right]^{1/2}$$

where

$$\left.\begin{aligned} T_1 &= Q_J\ K + Q_W(X_A + X_B + K) \\ T_2 &= T_1^{\,2} - 4\ Q_J\ Q_W\ K(X_A + X_B) \end{aligned}\right] \qquad (30)$$

Because the squeeze-film forces were obtained by an asymptotic approximation, there is no damping in the system. Consequently, ϵ and δ would become infinite when ω approaches ω_{cr}. Note that the critical frequencies given by (30) are independent of the squeeze mode function $b(\varphi)$. This is obviously due to the fact that we have linearized the system according to (24) which imposes the condition that both ϵ and $b(\varphi)$ must be small.

Actually, one can include the non-linear squeeze-film action in the critical frequency calculation by linearing with respect to ϵ. This can be easily achieved by starting with Eqs. (33), (34) and (35). One can write

$$\left.\begin{aligned} Z_A(\epsilon) &= Z_A(o) + \epsilon\ \alpha_A \\ Z_B(\epsilon) &= Z_B(o) + \epsilon\ \alpha_B \end{aligned}\right. \qquad (31)$$

Note that $Z_A(o)$, $Z_B(o)$, α_A and α_B are functions of $b(\varphi)$; or they do include the non-linear squeeze action. Following the same derivation one can show that the critical frequencies are given by

$$\omega_{cr} = \left[\frac{T_3 \pm \sqrt{T_4}}{2Q_J\ Q_W}\right]^{1/2}$$

where

$$\left.\begin{aligned} T_3 &= Q_J\ K + Q_W\ (-\alpha_A - \alpha_B + K) \\ T_4 &= T_3^{\,2} - 4\ Q_J\ Q_W\ K\ (-\alpha_A - \alpha_B) \end{aligned}\right. \qquad (32)$$

Non-linear Solution

Perform the τ integrations in Eq. (21) and rewrite Eq. (22).

$$(-B_J + K)\,\epsilon - Z_A(\epsilon) - Z_B(\epsilon) - K\,\delta = 0 \tag{33}$$

$$-K\,\epsilon + (-B_W + K)\,\delta = 0 \tag{34}$$

where

$$\left.\begin{aligned} Z_A(\epsilon) &= 2\int_{\varphi_1}^{\varphi_2} \frac{\psi_{\infty A}\sin 2\varphi}{\epsilon\cos\varphi - b(\varphi)}\left[1 - \frac{H_{oA}}{\sqrt{H_{oA}^2 - [\epsilon\cos\varphi - b(\varphi)]^2}}\right] d\varphi \\ Z_B(\epsilon) &= -2\int_{\varphi_1}^{\varphi_2} \frac{\psi_{\infty B}\sin 2\varphi}{-\epsilon\cos\varphi - b(\varphi)}\left[1 - \frac{H_{oB}}{\sqrt{H_{oB}^2 - [\epsilon\cos\varphi + b(\varphi)]^2}}\right] d\varphi \end{aligned}\right\} \tag{35}$$

Let ϵ_i and δ_i be the i-th iterated solution. To obtain the next improved solution ϵ_{i+1} and δ_{i+1}, let us denote the corrections by $\Delta\epsilon_i$ and $\Delta\delta_i$, or

$$\left.\begin{aligned} \epsilon_{i+1} &= \epsilon_i + \Delta\epsilon_i \\ \delta_{i+1} &= \delta_i + \Delta\delta_i \end{aligned}\right] \tag{36}$$

Since ϵ_{i+1} and δ_{i+1} must satisfy (33) and (34) we have

$$(-B_J + K)\,\epsilon_{i+1} - Z_A(\epsilon_{i+1}) - Z_B(\epsilon_{i+1}) - K\,\delta_{i+1} = 0 \tag{37}$$

$$-K\,\epsilon_{i+1} + (-B_W + K)\,\delta_{i+1} = 0 \tag{38}$$

Using Taylor's series expansion and taking only the first-order terms, we have

$$\left.\begin{aligned} Z_A(\epsilon_{i+1}) &= Z_A(\epsilon_i + \Delta\epsilon_i) = Z_A(\epsilon_i) + Z_A'(\epsilon_i)\,\Delta\epsilon_i \\ Z_B(\epsilon_{i+1}) &= Z_B(\epsilon_i) + Z_B'(\epsilon_i)\,\Delta\epsilon_i \end{aligned}\right] \tag{39}$$

Substitute (36) and (39) into (37) and (38) and solve for $\Delta\epsilon_i$ and $\Delta\delta_i$,

$$\begin{bmatrix} \Delta\epsilon_i \\ \Delta\delta_i \end{bmatrix} = \begin{bmatrix} -B_J + K - Z_A'(\epsilon_i) - Z_B'(\epsilon_i) & -K \\ -K & -B_W + K \end{bmatrix}^{-1} \begin{bmatrix} u_i \\ v_i \end{bmatrix} \tag{40}$$

where

$$\begin{aligned} u_i &= (B_J - K)\,\epsilon_i + Z_A(\epsilon_i) + Z_B(\epsilon_i) + K\,\delta_i \\ v_i &= (B_W - K)\,\delta_i + K\,\epsilon_i \end{aligned} \tag{41}$$

The iterative process indicated above can be repeated until both $\Delta\epsilon_i$ and $\Delta\delta_i$ are smaller than a specified value. The converged values of ϵ and δ are the solutions of (33) and (34).

3. LOAD CAPACITIES AND STIFFNESSES

Integrating the instantaneous squeeze-film forces given by (17) and (18) over one squeeze cycle, we have the time-average forces,

$$F_{zA} = \frac{1}{2\pi} \int_0^{2\pi} F_{IA}\, d\tau$$

$$F_{zB} = \frac{1}{2\pi} \int_0^{2\pi} F_{IB}\, d\tau \qquad (42)$$

or

$$\bar{F}_{zA} = \frac{F_{zA}}{\pi R^2 p_a} = \int_{\varphi_1}^{\varphi_2} \frac{\psi_{\infty A} \sin 2\varphi\, d\varphi}{\sqrt{H_{oA}^2 - [\varepsilon \cos \varphi - b(\varphi)]^2}}$$

$$+ \frac{1}{2} [\cos 2\varphi_2 - \cos 2\varphi_1] \qquad (43)$$

$$\bar{F}_{zB} = \frac{F_{zb}}{\pi R^2 p_a} = -\int_{\varphi_1}^{\varphi_2} \frac{\psi_{\infty B} \sin 2\varphi\, d\varphi}{\sqrt{H_{oB}^2 - [\varepsilon \cos \varphi + b(\varphi)]^2}}$$

$$- \frac{1}{2} [\cos 2\varphi_2 - \cos 2\varphi_1] \qquad (44)$$

The dimensionless load capacity is therefore

$$\bar{F}_z = \bar{F}_{zA} + \bar{F}_{zB} = \int_{\varphi_1}^{\varphi_2} \frac{\psi_{\infty A} \sin 2\varphi \, d\varphi}{\sqrt{H_{oA}^2 - [\epsilon \cos \varphi - b(\varphi)]^2}}$$

$$- \int_{\varphi_1}^{\varphi_2} \frac{\psi_{\infty B} \sin 2\varphi \, d\varphi}{\sqrt{H_{oB}^2 - [\epsilon \cos \varphi + b(\varphi)]^2}} \tag{45}$$

Thus, from (43), (44) and (45) it is clear how the squeeze-film forces are affected by the synchronous response of the float. In fact, it is a convenient concept to combine the (driving) squeeze motion and the synchronous response into an effective squeeze motion. The effective squeeze motion for bearing surface "A" is $\epsilon \cos \varphi - b(\varphi)$, and for bearing surface "B", $\epsilon \cos \varphi + b(\varphi)$. Previous analysis neglecting the synchronous response [4] is obviously a special case of the present analysis with $\epsilon = 0$.

The bearing stiffness can be obtained numerically by taking the difference between the forces at $\eta_A - \Delta\eta_A$ and $\eta_A + \Delta\eta_A$ for the bearing surface "A". Let $\Delta\eta_A = 0.01$, then

$$\bar{k}_{zA} = \frac{\bar{F}_{zA}(\eta_A - 0.01) - \bar{F}_{zA}(\eta_A + 0.01)}{0.02} \tag{46}$$

Similarly,

$$\bar{k}_{zB} = \frac{\bar{F}_{zB}(\eta_B - 0.01) - \bar{F}_{zB}(\eta_B + 0.01)}{0.02} \tag{47}$$

The dimensionless bearing stiffness is the sum of $\bar{k}_{zA}$ and $\bar{k}_{zB}$.

$$\bar{k}_z = \bar{k}_{zA} + \bar{k}_{zB} \tag{48}$$

and

$$\bar{k}_z = \frac{k_z C}{\pi R^2 p_a} \tag{49}$$

Both $\bar{F}_z$ and $\bar{k}_z$ are dependent on the synchronous response. We will use subscript "0" for those with $\epsilon = 0$, subscript "L" for $\bar{F}_z$ and $\bar{k}_z$ with ϵ given by the linearized solution, and subscript "N" for $\bar{F}_z$ and $\bar{k}_z$ with ϵ given by the non-linear solution.

4. RESULTS

An example of the spherical bearing system with the following input data will be considered.

$R = 2.67$ in.

$C = 0.001$ in.

$\varphi_1 = 36.5°$

$\varphi_2 = 70°$

$k = 0.5 \times 10^6$ lb/in.

$M_J = 2.0$ lb.

$M_W = 0.2$ lb.

$\eta_A = 0.2$

$\eta_B = 0.2$

Assume that the transducer can provide a uniform axial excursion throughout the whole frequency spectrum*. Thus, $b(\varphi) = \epsilon_1 \cos \varphi$ and assume $\epsilon_1 = 0.4$.

With the above input data, the responses ϵ and δ, as solved from (33) and (34), are plotted against ω in Figures 3 and 4. It is seen that ϵ and δ become infinite at both of the two critical frequencies, $\omega_{cr} = 32640$ rad/sec. and 7150 rad/sec.

The values of δ and of ϵ can be positive or negative depending on the squeeze frequency. Actually, the sign of δ is of no importance; it is the magnitude of δ that should be kept sufficiently small. On the other hand, ϵ is preferably positive. Because,with $\eta_A = \eta_B = 0.2$, and $H_{oB} < H_{oA}$, an increase of

---

* In reality, once the geometry of the transducer and the bearing structure are chosen, only a discrete number of frequencies corresponding to the natural modes of the system can be excited.

squeeze action in bearing "B" due to ϵ will be predominating. In order to achieve this, ϵ should be positive as can be seen from Eq. (45). A plot of $(\bar{F}_z)_N/(\bar{F}_z)_o$ and $(\bar{k}_z)_N/(\bar{k}_z)_o$ against ω is shown in Fig. 5. The effects of synchronous response on the load carrying capacity and stiffness are clearly depicted. $(\bar{F}_z)_N/(\bar{F}_z)_o$ is greater than unity whenever ϵ is positive. Although it seems desirable to operate the bearing at, say, ω = 10,000 rad/sec. to take advantage of the positive ϵ which results in a larger load capacity, an examination of δ from Fig. 4 indicates that δ = 0.06 which corresponds to a wheel vibration amplitude of 60 microinches (for C = 0.001 in.) If the actual application cannot tolerate such vibration amplitude, then it is desirable to design the squeeze frequency to be at least two or three times of the higher critical frequency. There, the float response ϵ would be negligibly small so that $(\bar{F}_z)_N/(\bar{F}_z)_o$ is practically unity and δ = .006 (wheel amplitude = 0.6 microinch for C = 0.001 in.) at ω = 70,000 rad/sec. The dimensionless wheel amplitude δ can be made even smaller by increasing ω.

In Fig. 6 the critical frequency of the system is plotted against k for the given bearing geometry ($\varphi_1 = 36.5°$, $\varphi_2 = 70°$, R = 2.67, $\eta_A = \eta_B = 0.2$) and M_J = 2 lb., M_W = 0.2 lb., $b(\varphi) = \epsilon_1 \cos\varphi$ and $\epsilon_1 = 0.4$.

Another set of data is generated by setting M_J = 6.5 lb. and M_W = 0.5 lb. (and keeping the same φ_1, φ_2 and R) which represents an actual squeeze-film bearing design for NASA [ ]. The results shown in Figures 7 to 10 are qualitatively the same as those of the previous bearing shown in Figures 3 to 6.

The analysis of the two-mass conical bearing system is included in Appendix I. A computer program has also been written. The numerical results for the conical bearing system are quite similar to the spherical bearing system and are therefore, not included in this report.

So far, we have considered spherical bearing system with uniform axial squeeze motion. But, if the transducer of a squeeze-film bearing is operated at high frequencies, it often produces non-uniform squeeze motion which represents higher modes of vibration of the transducer structure. Recall that $b(\varphi)$ is the

normal component of the dimensionless squeeze amplitude. In Fig. 11, the $b(\varphi)$ of a transducer designed for NASA , is depicted. This $b(\varphi)$ is the normal mode of the structure at 25.2 khz. Using the $b(\varphi)$ of Fig. 11 as an input and setting M_J = 6 lb., M_W = 0.5 lb. and the same bearing geometry we can use the computer program to calculate the responses ϵ and δ. Since it is known that the critical frequencies of the bearing system should be low compared to the squeeze frequency (25.2 khz), we plot the critical frequencies against k in Fig. 12. It is seen that for k = 0.5×10^6 lb/in., the two critical frequencies are 20,000 rad/sec. and 4500 rad/sec. Since the squeeze frequency is 25.2 khz (or 158,000 rad/sec.), it can be concluded that for the particular squeeze-film system under consideration, the amplitudes of the synchronous responses, ϵ and δ, are negligibly small.

5. SUMMARY AND CONCLUSIONS

Synchronous responses of spherical and conical squeeze-film bearing systems were analyzed theoretically based on the method of a harmonic analysis developed in Ref. 9. The two-mass model was motivated by the special application of the gimbal suspension of a gyro. The responses of both the float (the journal) and the gyro wheel were considered.

Based on the results obtained, the following conclusions can be drawn:

1. The responses of the journal and the wheel show typical behavior of the dynamic response of a two degree-of-freedom system. Two critical frequencies can be calculated from the analysis.

2. The response of the journal may result in appreciably higher load capacity and stiffness in certain squeeze frequency range. However, one cannot take advantage of this high load capacity because at those frequencies the response of the wheel becomes excessive.

3. When the squeeze frequency is much higher than the critical frequencies, both the journal and the wheel responses have negligibly small amplitudes; the load capacity and stiffness are practically not affected by the synchronous responses.

4. Since the wheel excitation is generally not desirable, the squeeze frequency should be designed to be sufficiently higher than the critical frequencies.

APPENDIX I - Analysis for Conical Bearing System

In a conical coordinate system, r is measured from the apex of a cone as shown in Fig. 2. For the case of a radially unloaded bearing we do not have to consider the cyclic coordinate. The analysis we shall formulate here is very similar to the spherical bearing as can be anticipated. The normalized film thicknesses for the conical bearings are

$$H_A = 1 + \eta_A \sin \Gamma + [\epsilon \sin \Gamma - b(\zeta)] \cos \tau \tag{I.1}$$

$$H_B = 1 - \eta_B \sin \Gamma + [-\epsilon \sin \Gamma - b(\zeta)] \cos \tau \tag{I.2}$$

where Γ is the half cone angle, ϵ is the journal dynamic response $b(\zeta)$ is the squeeze mode function and $\zeta = r/R$. For uniform axial squeezing with amplitude ϵ_1, $b(\zeta) = \epsilon_1 \sin \Gamma$.

The asymptotic approximations of PH for the conical bearings can be easily obtained. The derivation is quite similar to the spherical bearing and is omitted here. The results can be written down as follows.

$$\psi_{\infty A} = (1 + \eta_A \sin \Gamma) \sqrt{F_A(\zeta)} \tag{I.3}$$

$$\psi_{\infty B} = (1 - \eta_B \sin \Gamma) \sqrt{F_B(\zeta)} \tag{I.4}$$

where

$$
\left.
\begin{aligned}
F_A(\zeta) &= E_A \frac{1}{H_{oA}^3} \ell n \frac{\zeta}{\zeta_1} + F_A(\zeta_1) \\
E_A &= \frac{F_A(\zeta_2) - F_A(\zeta_1)}{\frac{1}{H_{oA}^3} \ell n \frac{\zeta_2}{\zeta_1}} \\
F_A(\zeta_2) &= 1 + \frac{3}{2} \left[\frac{\epsilon \sin \Gamma - b(\zeta_2)}{H_{oA}} \right]^2 \\
F_A(\zeta_1) &= 1 + \frac{3}{2} \left[\frac{\epsilon \sin \Gamma - b(\zeta_1)}{H_{oA}} \right]^2 \\
H_{oA} &= 1 + \eta_A \sin \Gamma
\end{aligned}
\right\} \qquad \text{(I.5)}
$$

and

$$
\left.
\begin{aligned}
F_B(\zeta) &= E_B \frac{1}{H_{oB}^3} \ell n \frac{\zeta}{\zeta_1} + F_B(\zeta_1) \\
E_B &= \frac{F_B(\zeta_2) - F_B(\zeta_1)}{\frac{1}{H_{oB}^3} \ell n \frac{\zeta_2}{\zeta_1}} \\
F_B(\zeta_2) &= 1 + \frac{3}{2} \left[\frac{\epsilon \sin \Gamma + b(\zeta_2)}{H_{oB}} \right]^2 \\
F_B(\zeta_1) &= 1 + \frac{3}{2} \left[\frac{\epsilon \sin \Gamma + b(\zeta_1)}{H_{oB}} \right]^2 \\
H_{oB} &= 1 - \eta_B \sin \Gamma
\end{aligned}
\right\} \qquad \text{(I.6)}
$$

The axial instantaneous film forces are

$$\frac{F_{IA}}{\pi R^2 p_a} = 2 \sin^2 \Gamma \int_{\zeta_1}^{\zeta_2} \frac{\psi_{\infty A} \zeta \, d\zeta}{H_{oA} + [\epsilon \sin \Gamma - b(\zeta)] \cos \tau} - \sin^2 \Gamma (\zeta_2^2 - \zeta_1^2)$$

$$\frac{F_{IB}}{\pi R^2 p_a} = -2 \sin^2 \Gamma \int_{\zeta_1}^{\zeta_2} \frac{\psi_{\infty B} \zeta \, d\zeta}{H_{oB} + [-\epsilon \sin \Gamma - b(\zeta)] \cos \tau} + \sin^2 \Gamma (\zeta_2^2 - \zeta_1^2)$$

We can write the equations of motion of the journal and of the wheel.

$$- M_J C \epsilon \omega^2 \cos \tau = F_{IA} + F_{IB} - kC (\epsilon - \delta) \cos \tau - W_J - W_W \qquad (I.7)$$

$$- M_W C \delta \omega^2 \cos \tau = kC (\epsilon - \delta) \cos \tau \qquad (I.8)$$

Multiply (I.7) and (I.8) by cos τ and integrate from 0 to 2π,

$$- B_J \epsilon = \frac{2 \sin^2 \Gamma}{\pi} \int_{\zeta_1}^{\zeta_2} d\zeta \int_0^{2\pi} \frac{(\psi_{\infty A} \zeta) \cos \tau \, d\tau}{H_{oA} + [\epsilon \sin \Gamma - b(\zeta)] \cos \tau}$$

$$- \frac{2 \sin^2 \Gamma}{\pi} \int_{\zeta_1}^{\zeta_2} d\zeta \int_0^{2\pi} \frac{(\psi_{\infty B} \zeta) \cos \tau \, d\tau}{H_{oB} + [-\epsilon \sin \Gamma - b(\zeta)] \cos \tau} - K (\epsilon - \delta) \qquad (I.9)$$

$$- B_W \epsilon = K (\epsilon - \delta) \qquad (I.10)$$

where

$$B_J = \frac{M_J C \omega^2}{386\, p_a \pi R^2}$$

$$B_W = \frac{M_W C \omega^2}{386\, p_a \pi R^2}$$

$$K = \frac{kC}{p_a \pi R^2}$$

Linearized Solution

If $\frac{\epsilon \sin \Gamma - b}{H_{oA}} \ll 1$ and $\frac{\epsilon \sin \Gamma + b}{H_{oB}} \ll 1$

then from (I.9) and (I.10), we have

$$\begin{cases} -B_J \epsilon = 2 \sin^2 \Gamma \int_{\zeta_1}^{\zeta_2} \frac{(\psi_{\infty A}\zeta)\,[-\epsilon \sin \Gamma + b(\zeta)]}{H_{oA}^2}\, d\zeta \\ \qquad\qquad - 2 \sin^2 \Gamma \int_{\zeta_1}^{\zeta_2} \frac{(\psi_{\infty B}\zeta)\,[\epsilon \sin \Gamma + b(\zeta)]}{H_{oB}^2}\, d\zeta - K(\epsilon - \delta) \\ -B_M \delta = K(\epsilon - \delta) \end{cases}$$

or

$$\begin{cases} -B_J \epsilon + X_A \epsilon + X_B \epsilon + K\epsilon - K\delta = Y_A + Y_B & \text{(I.11)} \\ -B_W \delta + K\delta - K\epsilon = 0 & \text{(I.12)} \end{cases}$$

where

$$\left.\begin{aligned} X_A &= \frac{\sin^3 \Gamma}{H_{oA}} \left(\zeta_2^2 - \zeta_1^2\right) \\ X_B &= \frac{\sin^3 \Gamma}{H_{oB}} \left(\zeta_2^2 - \zeta_1^2\right) \\ Y_A &= \frac{2 \sin^2 \Gamma}{H_{oA}} \int_{\zeta_1}^{\zeta_2} \zeta \, b\,(\zeta)\, d\zeta \\ Y_B &= -\frac{H_{oA}}{H_{oB}} Y_A \end{aligned}\right\} \qquad \text{(I.13)}$$

In matrix form we can write

$$\begin{bmatrix} (-B_J + X_A + X_B + K) & -K \\ -K & -B_W + K \end{bmatrix} \begin{bmatrix} \epsilon \\ \delta \end{bmatrix} = \begin{bmatrix} Y_A + Y_B \\ 0 \end{bmatrix}$$

Thus,

$$\begin{bmatrix} \epsilon \\ \delta \end{bmatrix} = \begin{bmatrix} (-B_J + X_A + X_B + K) & -K \\ -K & (-B_W + K) \end{bmatrix}^{-1} \begin{bmatrix} Y_A + Y_B \\ 0 \end{bmatrix} \qquad \text{(I.14)}$$

The critical frequencies can be obtained in a manner similar to (32),

$$\omega_{cr} = \left[\frac{T_3 + \sqrt{T_4}}{2 Q_J Q_W} \right] \qquad \text{(I.15)}$$

where

$$\left.\begin{aligned} T_3 &= Q_J K + Q_W (-\beta_A - \beta_B + K) \\ T_4 &= T_3^2 - 4 Q_J Q_W K (-\beta_A - \beta_B) \\ \beta_A &= \frac{W_A(\epsilon) - W_A(o)}{\epsilon} \\ \beta_B &= \frac{W_B(\epsilon) - W_B(o)}{\epsilon} \end{aligned}\right\} \qquad (I.16)$$

W_A and W_B are defined in expressions preceding Eq. (I.19)

Non-linear Solution

Carrying out the τ integration, we have

$$-B_J \epsilon = \frac{2\pi}{\pi} 2 \sin^2 \Gamma \int_{\zeta_1}^{\zeta_2} \frac{\psi_{\infty A} \zeta}{\epsilon \sin \Gamma - b(\zeta)} \left[1 - \frac{h_{oA}}{\sqrt{H_{oA}^2 - [\epsilon \sin \Gamma - b(\zeta)]^2}}\right] d\zeta$$

$$- \frac{2\pi}{\pi} 2 \sin^2 \Gamma \int_{\zeta_1}^{\zeta_2} \frac{\psi_{\infty B} \zeta}{-\epsilon \sin \Gamma - b(\zeta)} \left[1 - \frac{h_{oB}}{\sqrt{H_{oB}^2 - [\epsilon \sin \Gamma + b(\zeta)]^2}}\right] d\zeta$$

$$- K (\epsilon - \delta) \qquad (I.17)$$

$$-K_W \delta = K (\epsilon - \delta) \qquad (I.18)$$

Denote

$$W_A(\epsilon) = 4 \sin^2 \Gamma \int_{\zeta_1}^{\zeta_2} \frac{\psi_{\infty A} \zeta}{\epsilon \sin \Gamma - b(\zeta)} \left[1 - \frac{h_{oA}}{\sqrt{H_{oA}^2 - [\epsilon \sin \Gamma - b(\zeta)]^2}}\right] d\zeta$$

$$W_B(\epsilon) = -4 \sin^2 \Gamma \int_{\zeta_1}^{\zeta_2} \frac{\psi_{\infty B} \zeta}{-\epsilon \sin \Gamma - b(\zeta)} \left[1 - \frac{h_{oB}}{\sqrt{H_{oB}^2 - [\epsilon \sin \Gamma + b(\zeta)]^2}}\right] d\zeta$$

Then Eqs. (I.17) and (I.18) become

$$(-B_J + K)\,\epsilon - W_A(\epsilon) - W_B(\epsilon) - K\,\delta = 0 \qquad \text{(I.19)}$$

$$(-B_W + K)\,\delta - K\,\epsilon = 0 \qquad \text{(I.20)}$$

The iteration scheme used to solve Eqs. (33) and (34) can be utilized here to obtain the non-linear solutions ϵ and δ from (I.19) and (I.20).

Now, the time averaged squeeze-film forces are, by integrating the instantaneous squeeze forces over one squeeze cycle,

$$\bar{F}_{zA} = \frac{F_{zA}}{\pi R^2 p_a} = 2 \sin^2 \Gamma \int_{\zeta_1}^{\zeta_2} \frac{\psi_{\infty A} \zeta \, d\zeta}{\sqrt{H_{oA}^2 - [\epsilon \sin \Gamma - b(\zeta)]^2}} - \sin^2 \Gamma \,(\zeta_2^2 - \zeta_1^2) \qquad \text{(I.21)}$$

$$\bar{F}_{zB} = \frac{F_{zB}}{\pi R^2 p_a} = -2 \sin^2 \Gamma \int_{\zeta_1}^{\zeta_2} \frac{\psi_{\infty B} \zeta \, d\zeta}{\sqrt{H_{oB}^2 - [\epsilon \sin \Gamma + b(\zeta)]^2}} + \sin^2 \Gamma \,(\zeta_2^2 - \zeta_1^2) \qquad \text{(I.22)}$$

The dimensionless load capacity is therefore

$$\bar{F}_z = \bar{F}_{zA} + \bar{F}_{zB} \tag{I.23}$$

The dimensionless stiffness can be easily calculated by using Eqs. (46) to (49). All the numerical computations have been programmed on a computer.

A numerical example is considered here with the following input data.

$R = 2.55$ in.

$C = 0.011$ in.

$\zeta_1 = 0.85$

$\zeta_2 = 1.57$

$k = 0.5 \times 10^6$ lb/in.

$M_J = 2$ lb.

$M_W = 0.2$ lb.

$\Gamma = 39.5°$

$\eta_A = 0.2$

$\eta_B = 0.2$

$b(\zeta) = \epsilon_1 \sin \Gamma$

$\epsilon_1 = 0.4$

The above geometry was chosen to resemble the spherical bearing geometry. The numerical results are very similar to those of the spherical bearing system as can be anticipated; they are not included in this report.

REFERENCES

1. Salbu, E.O.J., "Compressible Squeeze Films and Squeeze Bearings," Journal of Basic Engineering, Trans. ASME, Series D, Vol. 86, 1964, pp. 355-366.

2. Pan, C.H.T., "On Asymptotic Analysis of Gaseous Squeeze-Film Bearings," Journal of Lubrication Technology, Trans. of ASME, Vol. 89, Series F, No. 3, July 1967, p. 245.

3. Pan, C.H.T., Malanoski, S.B., Broussard, Jr., P.H. and Burch, J.L.,"Theory and Experiments of Squeeze-Film Gas Bearings - Part 1 Cylindrical Journal Bearing," Journal Basic Eng., Trans. ASME, Vol. 88, Series D, No. 1, March 1966, p. 191.

4. Chiang, T., Malanoski, S. B. and Pan, C.H.T., "Spherical Squeeze-Film Hybrid Bearing with Small Steady-State Radial Displacement," Journal of Lubrication Technology, Trans. of ASME, Vol. 89, Series F, No. 3, July 1967, p. 254.

5. Malanoski, S. B. and Pan, C.H.T., "The Solution of Special Squeeze-Film Gas Bearing Problems by an Improved Numerical Technique," MTI Technical Report MTI-65TR26, Mechanical Technology Incorporated, Latham, New York, February 1966.

6. Beck, J. V. and Strodtman, C. L., "Load Support of the Squeeze-Film Journal Bearing of Finite Length," Journal of Lubrication Technology, Trans. ASME, Vol. 90, Series F, No. 1, January 1968, p. 157.

7. Pan, C.H.T. and Chiang, T., Discussion on [5], Journal of Lubrication Technology Trans. of ASME Vol. 90, Series F, to appear.

8. Beck, J. B., Holliday, W. G. and Strodtman, C. L., "Experiment and Analysis of a Flat Disk Squeeze-Film Bearing Including Effects of Supported Mass Motion," ASME 68-LubS-35.

9. Chiang, T., Pan, C.H.T., and Elrod, H.G., "Dynamic Response of a Double Squeeze-Film Thrust Plate," MTI Report 68TR56.

10. Pan, C.H.T. and Chiang, T., "Dynamic Behavior of Spherical Squeeze-Film Hybrid Bearing", Journal of Lubrication Technology, Trans. ASME, Vol. 91, Series F, No. 1, p. 149, 1969.

11. Elrod, H.G., "A Differential Equation for Dynamic Operation of Squeeze-Film Bearings", presented at the Third Bi-Annual Gas Bearing Symposium, University of Southampton, April 1967.

NOMENCLATURE

B	dimensionless mass parameter, defined in Eq. (23)
$b(\varphi)$	squeeze mode function
C	bearing clearance
E_A, E_B	defined in Eqs. (12) and (13)
$F(\varphi)$	defined in Eq. (8)
F_z	axial squeeze-film load capacity
$\bar{F}_z$	dimensionless F_z
H	bearing film thickness normalized with respect to C
H_o	time-average of H
k	stiffness of wheel bearings
k_z	axial squeeze-film stiffness
$\bar{k}_z$	dimensionless k_z
K	defined in Eq. (23)
M	mass
p	pressure
p_a	ambient pressure
P	p/p_a
R	radius of sphere or cone base
t	time
δ	amplitude of wheel response
ϵ	amplitude of journal response
η_A, η_B	journal displacements from respective concentric position, defined to be positive upwards

NOMENCLATURE (Continued)

μ	viscosity
σ	squeeze number
τ	dimensionless time, Ωt
φ	azimuthal angle in spherical coordinate
Ψ	PH
Ω	squeeze frequency

Subscripts

A,B	bearing (or journal) A and B
J	journal
L	pertaining to linearized harmonic solution
N	pertaining to non-linear harmonic solution
o	setting $\epsilon = 0$
W	wheel
∞	asymptotic approximation for $\sigma \rightarrow \infty$

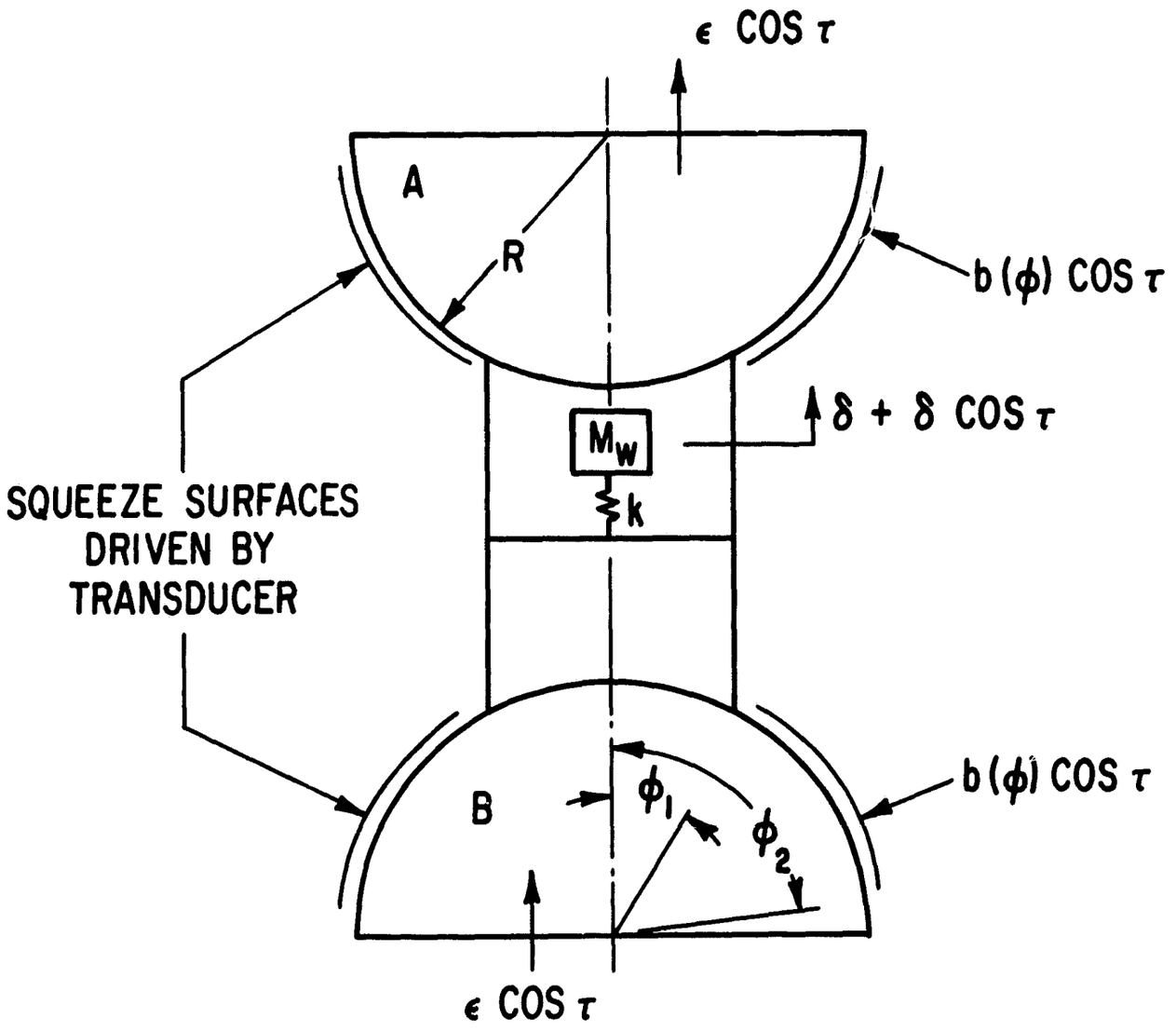

Fig. 1 Spherical Squeeze-Film Bearing System

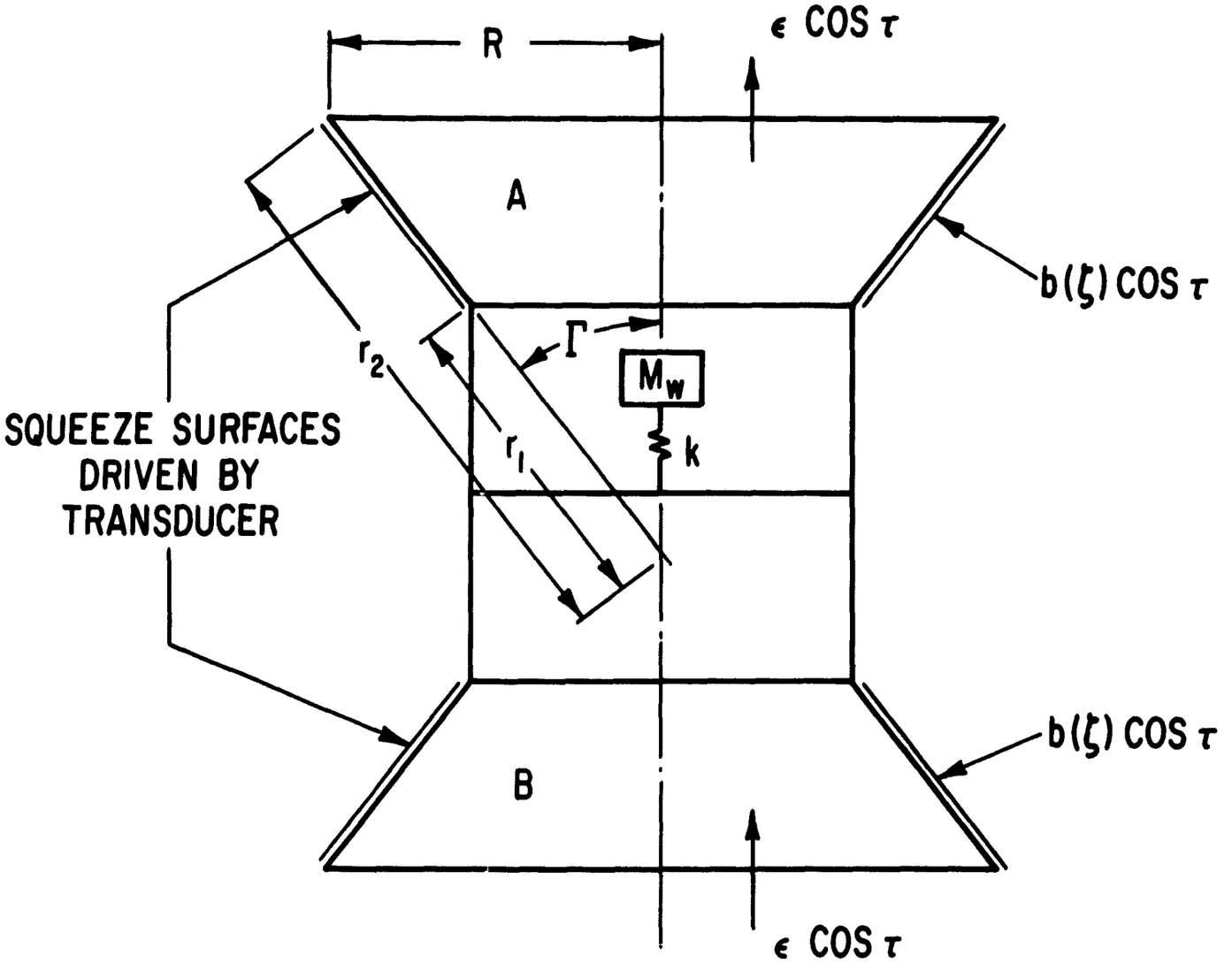

Fig. 2 Conical Squeeze-Film Bearing System

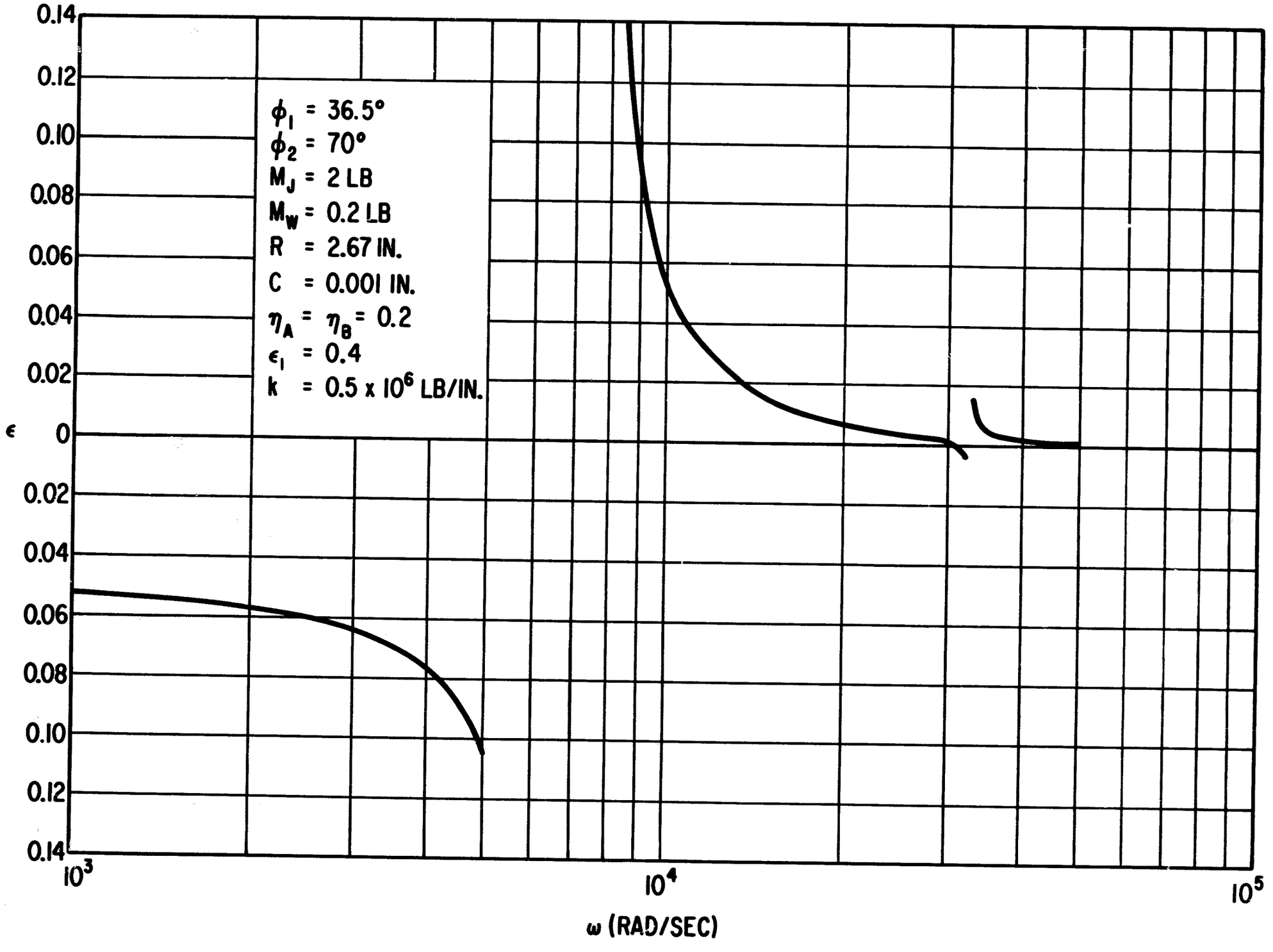

Fig. 3 Journal Response Amplitude Versus Frequency

MTI-6991

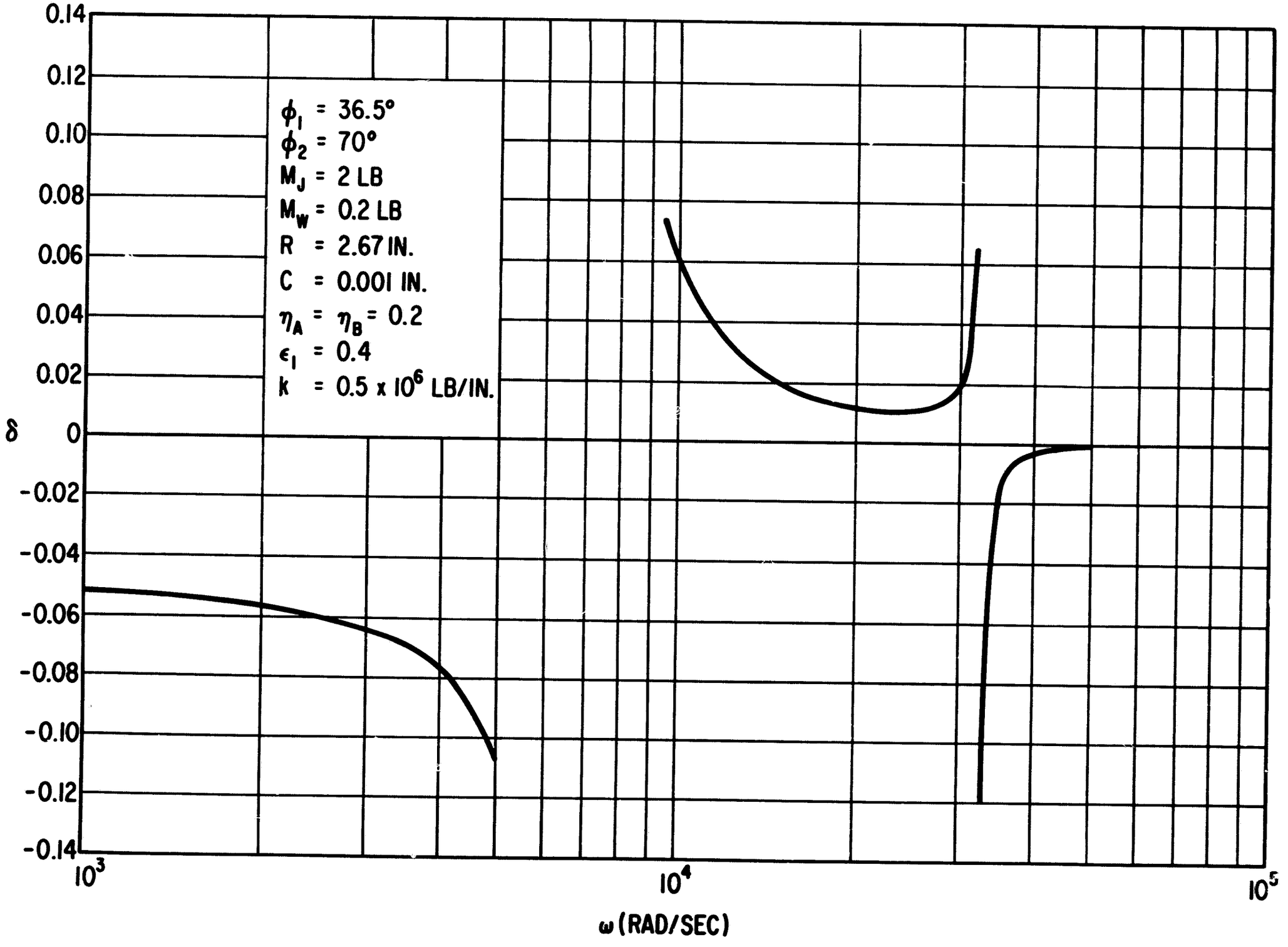

Fig. 4 Wheel Response Amplitude Versus Frequency

MTI-6989

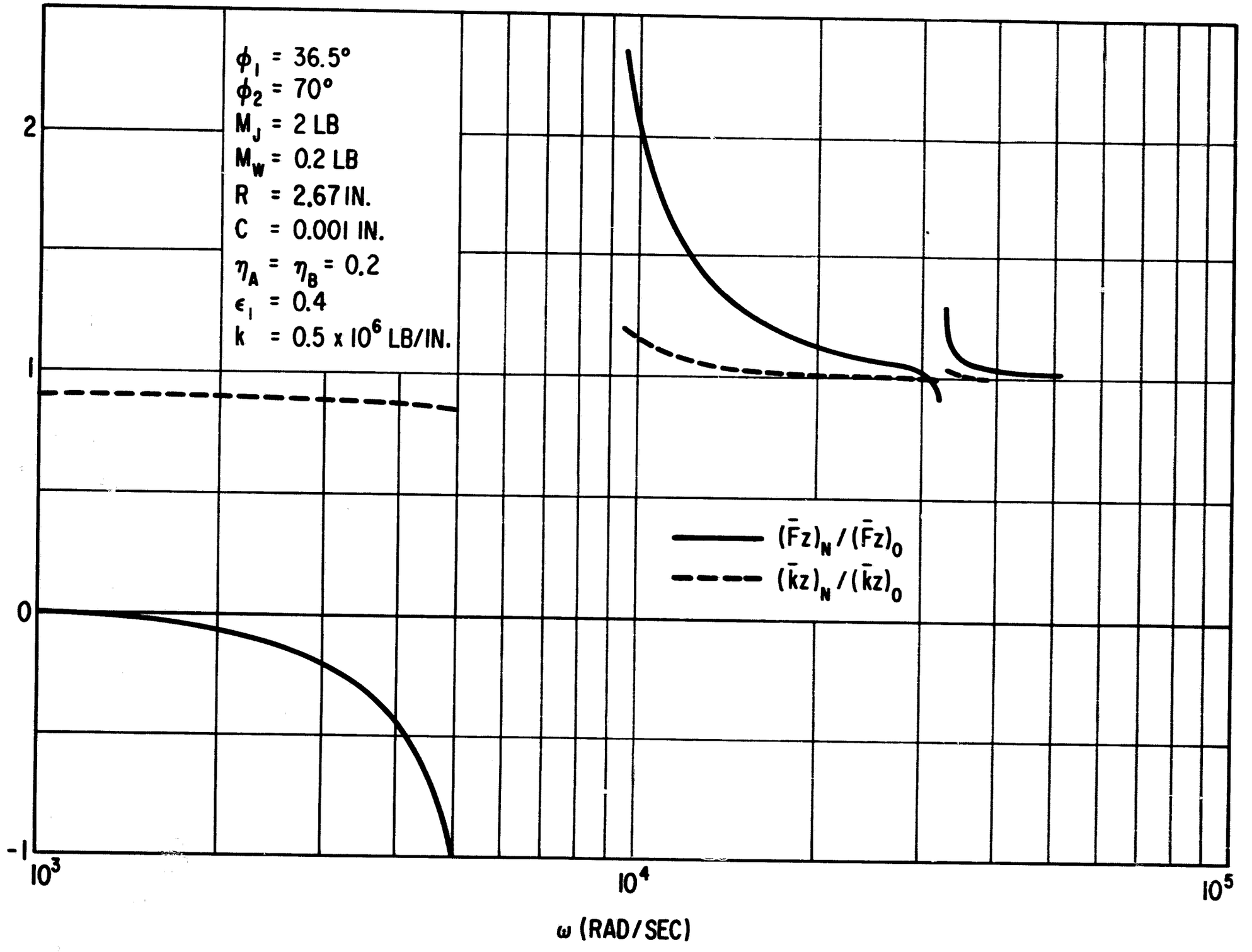

Fig. 5 Normalized Load Capacity and Stiffness Versus Frequency

MTI-6990

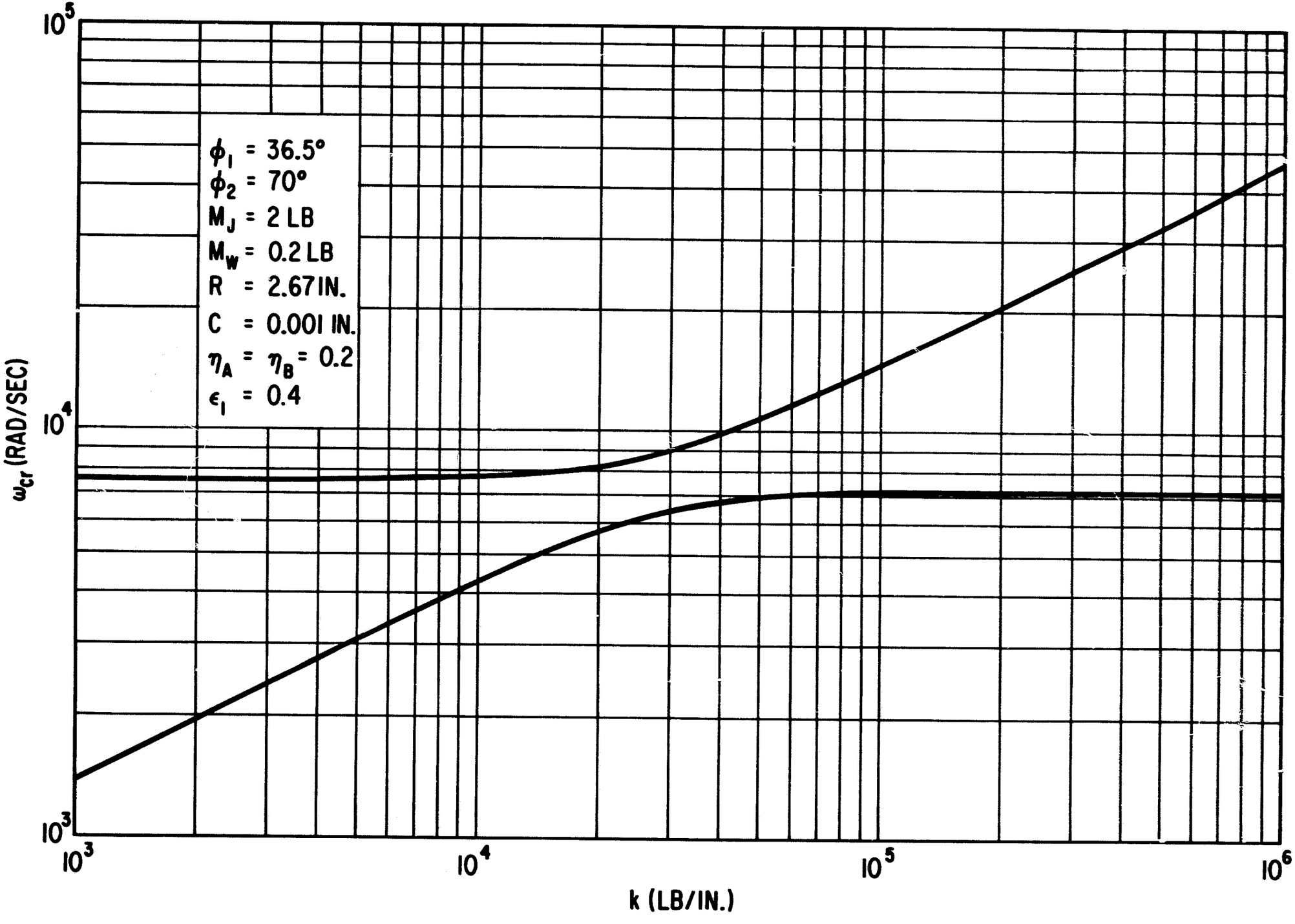

Fig. 6 Critical Frequencies Versus k.

MTI-6988

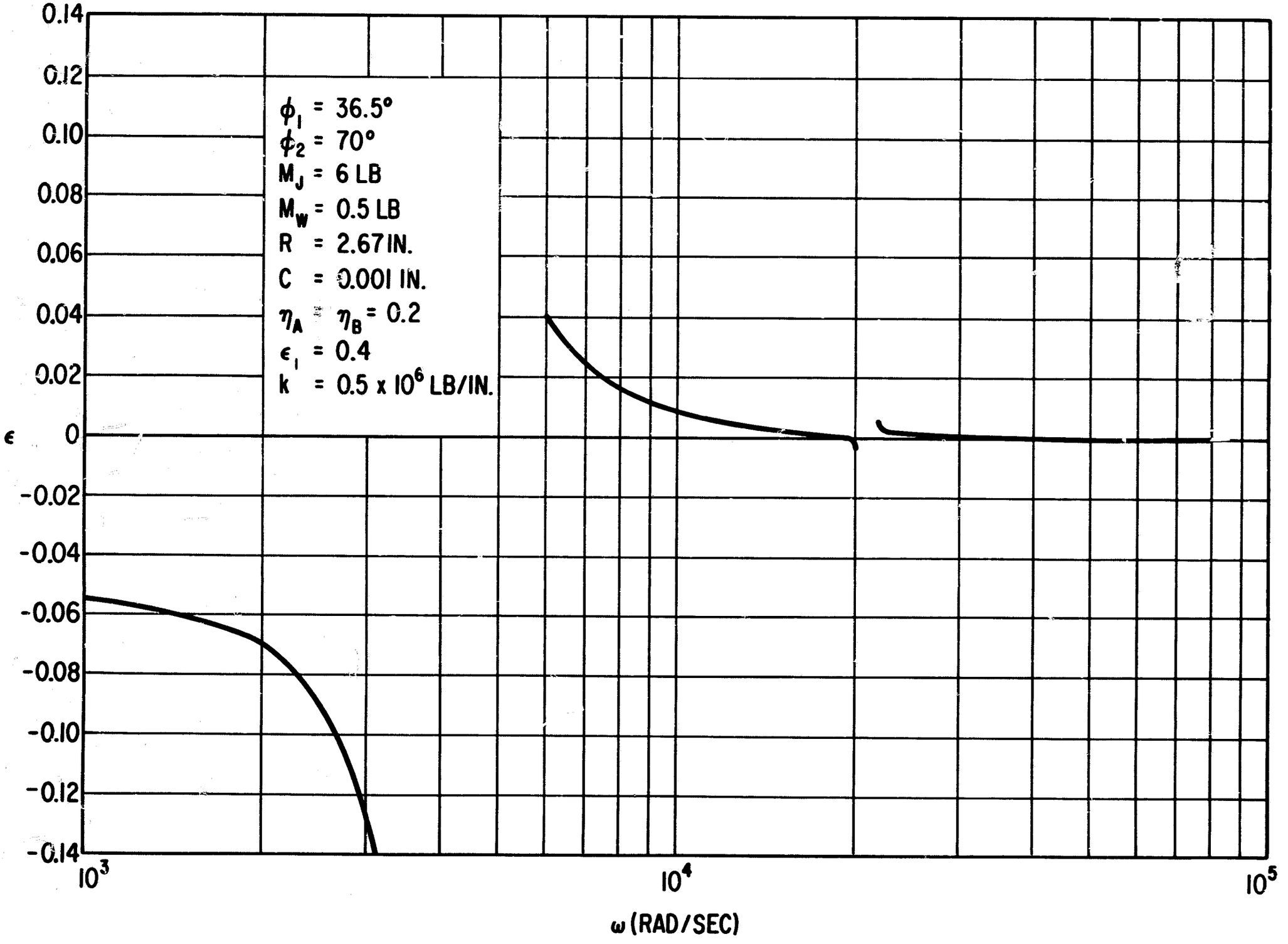

Fig. 7 Journal Response Amplitude Versus Frequency

MTI-6984

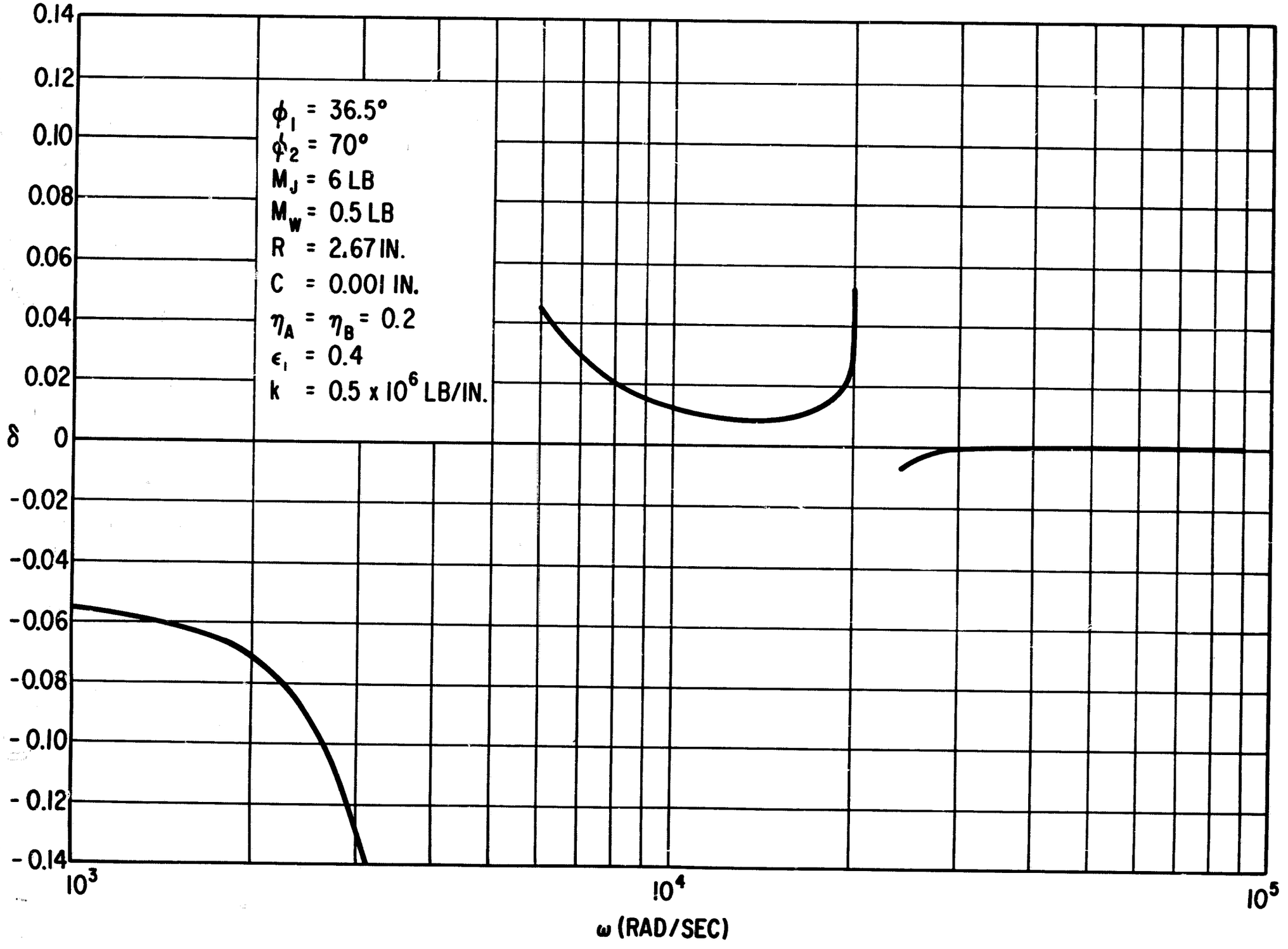

Fig. 8 Wheel Response Amplitude Versus Frequency

MTI-6986

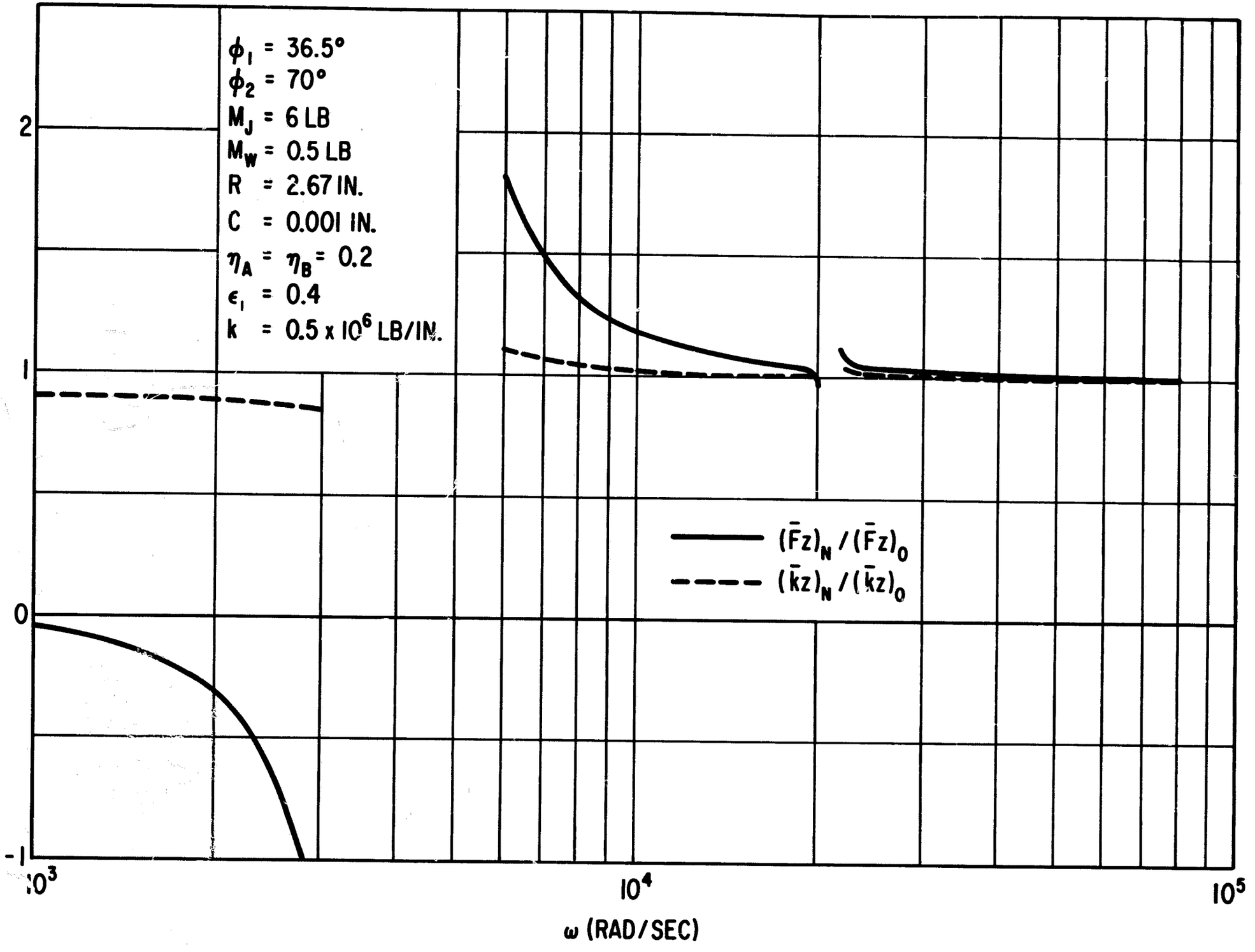

Fig. 9 Normalized Load Capacity and Stiffness Versus Frequency

MTI-6985

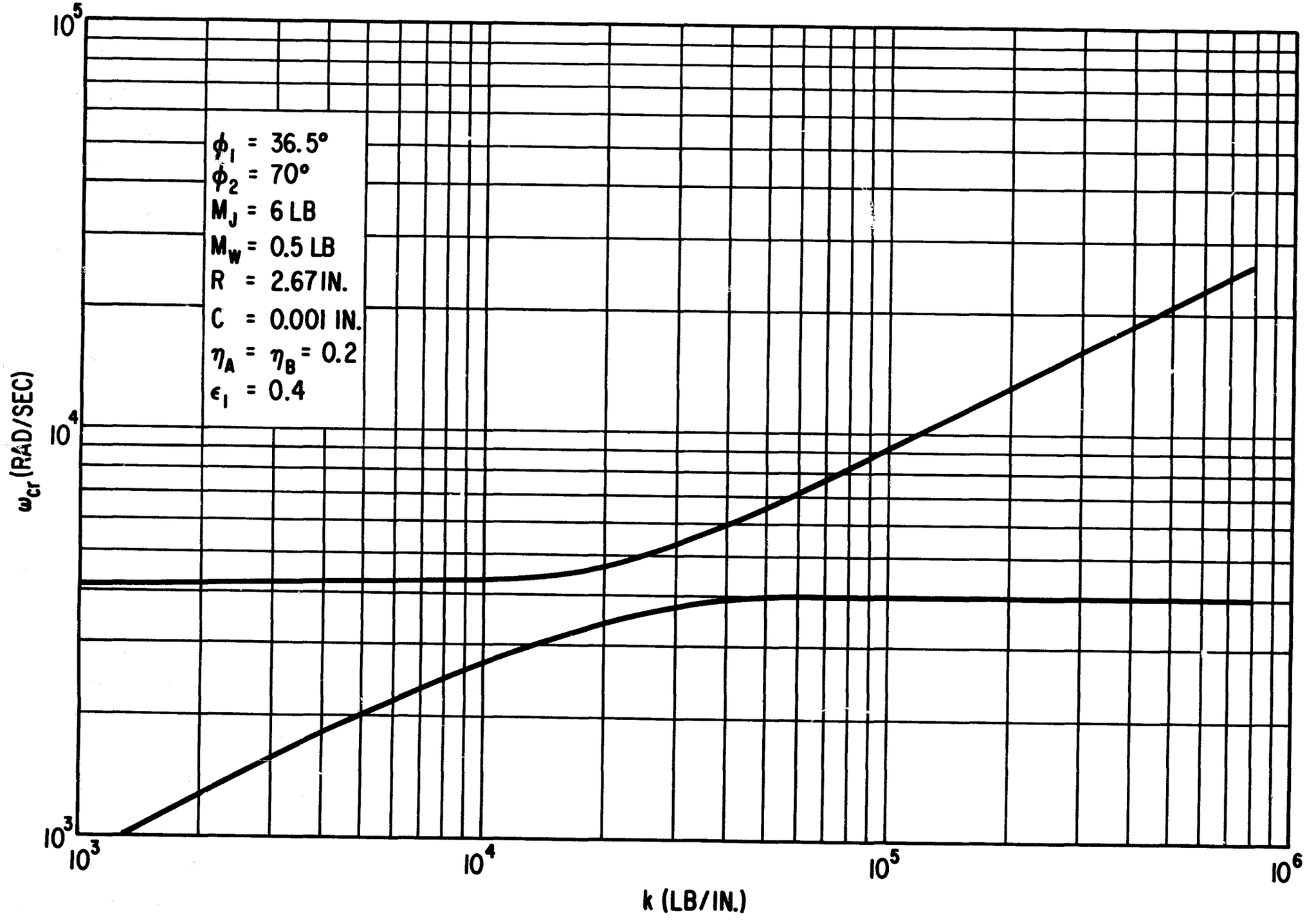

Fig. 10 Critical Frequencies Versus k

MTI-6981

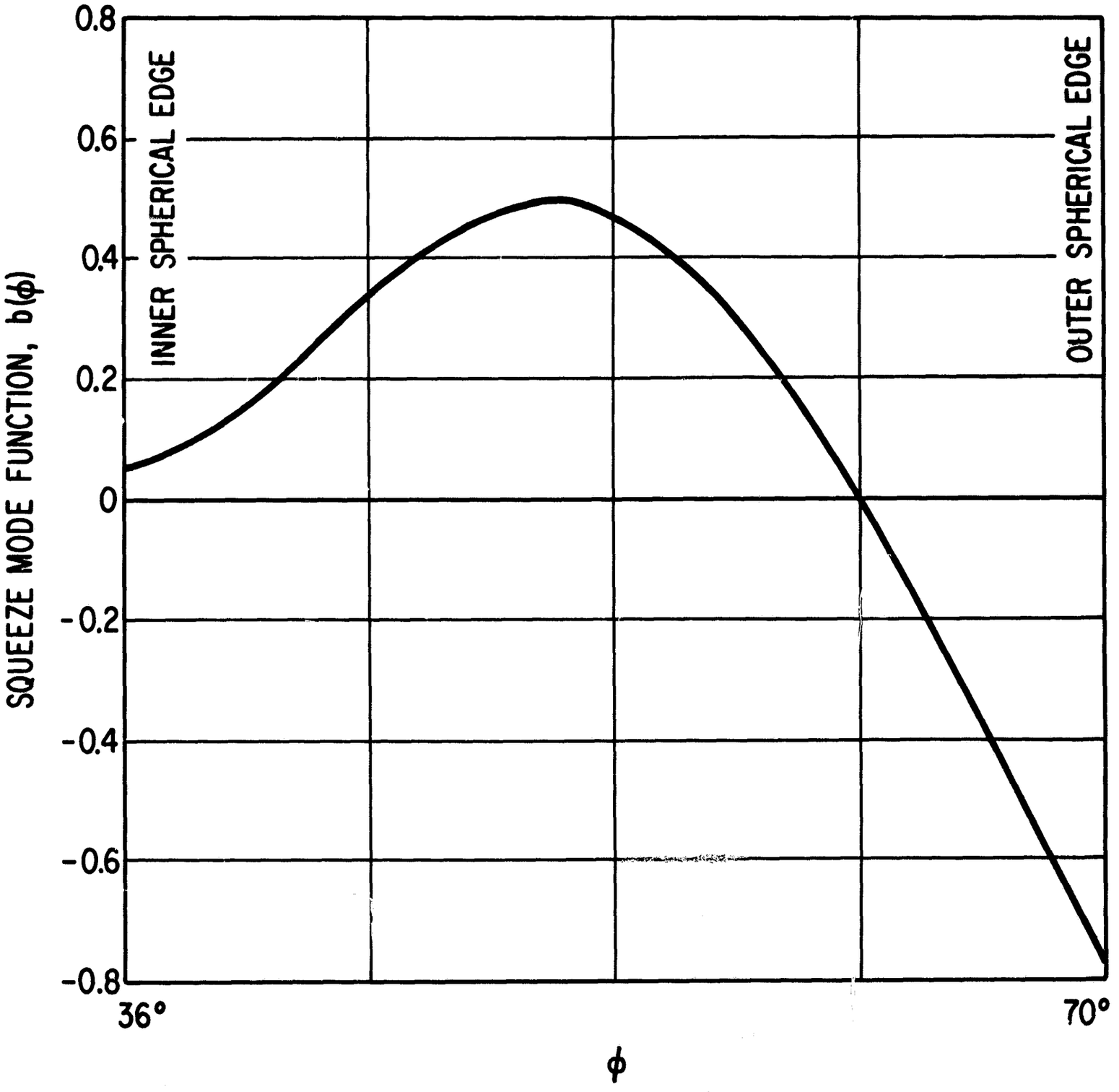

Fig. 11 Squeeze Mode Function Versus ϕ

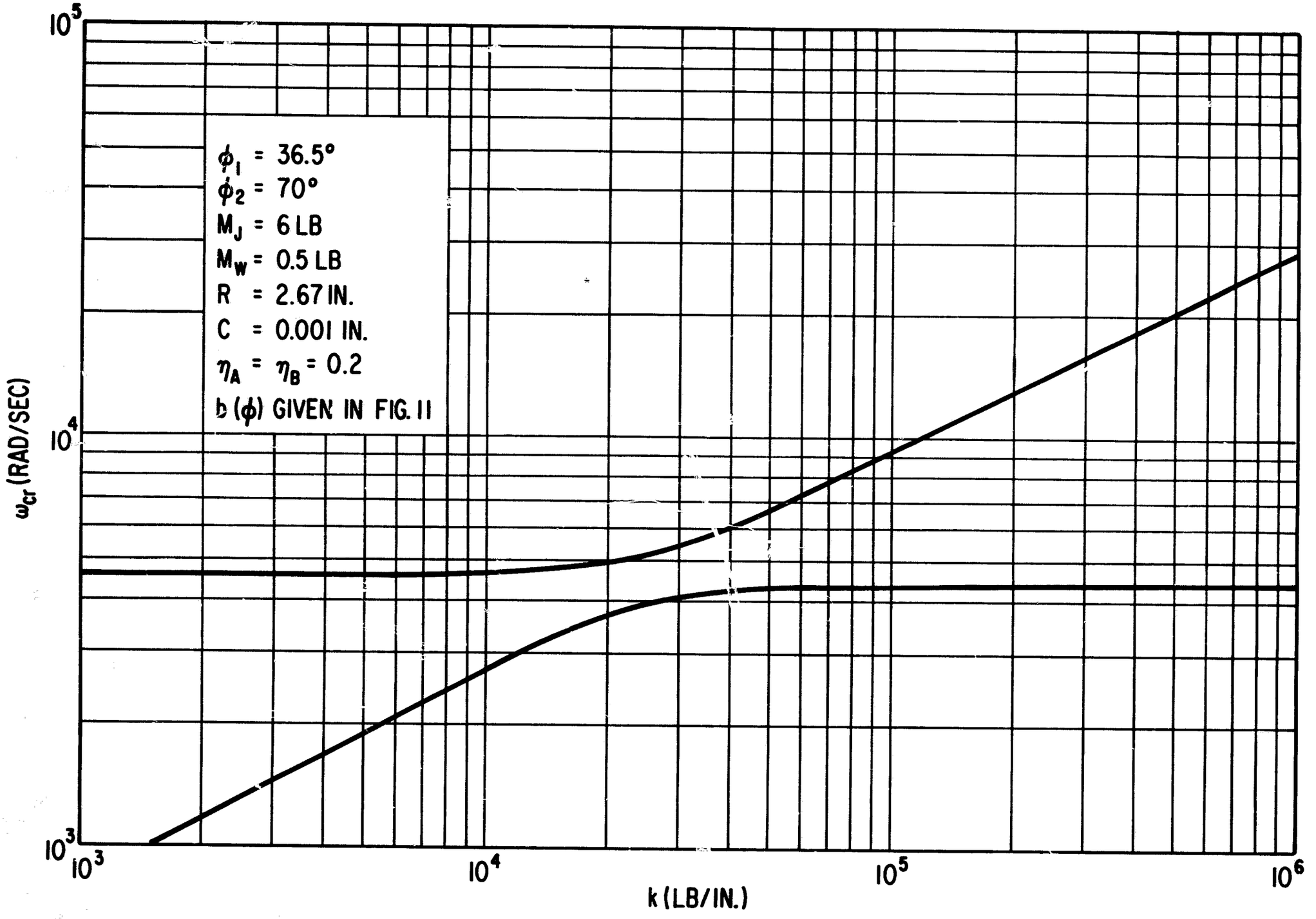

Fig. 12 Critical Frequencies Versus k with b(ϕ) given in Fig. 11

MTI-6987